Available online at www.sciencedirect.com
ScienceDirect
Ceramics International 37 (2011) 3665–3670
CERAMICS INTERNATIONAL
www.elsevier.com/locate/ceramint

New vanadium doped calcium titanate ceramic pigment

C. Gargori, S. Cerro, R. Galindo, A. García, M. Llusar, J. Badenes, G. Monrós *

Dpt. of Inorganic and Organic Chemistry, Jaume I University, Av. de Vicent Sos Baynat, s/n. 12071, Castellón, Spain

Received 2 June 2011; received in revised form 13 June 2011; accepted 14 June 2011
Available online 23 June 2011

Abstract

In this paper a new pink vanadium doped calcium titanate $Ca(V_xTi_{1-x})O_3$ ceramic pigment in conventional ceramic glazes is obtained by ceramic route and characterized. The limit of solid solution is near by $x = 0.2$, higher amounts of vanadium crystallizes $Ca_2V_2O_7$ which dilute the real amount of saturated $Ca(V_xTi_{1-x})O_3$ solid solution and diminish the intensity of colour. The unit cell parameter measurements of $Ca(V_xTi_{1-x})O_3$ agrees with the substitution of Ti^{4+} by V^{5+} that is associated to a V^{5+}–$O^{=}$ charge transfer at 420 nm on UV–vis–NIR spectra of 5% glazed samples that explain the pink colour obtained. In order to avoid the limitation due to the suppressing of oxygen vacancies by high valence cation V^{5+} substitution in a Ti^{4+} site of $CaTiO_3$ perovskite for to preserve the charge neutrality of the lattice; Fe^{3+} and V^{5+} codoped samples $Ca(Fe_xV_xTi_{1-2x})O_3$ $x = 0.1$, 0.2 and 0.3 were prepared and show a brown colour fired 1000 °C, but 5% glazed do not produce colour indicating that iron codoping inhibits the pigmenting capacity of vanadium doped $CaTiO_3$ perovskite.

Keywords: D. Perovskite; Ceramic pigment; Vanadium

1. Introduction

Perovskite ABO_3 is an ideally cubic phase, but really becomes a rhombic syngony (space group Pnma). A cation (Ca^{2+}, Sr^{2+}, Cd^{2+}, Ba^{2+}, Ni^{2+}, Co^{2+}) ideally occupies vertex of cube and B cation (Ti^{4+}, Zr^{4+}, Sn^{4+}) the centre, oxygen occupy face centres. Several authors have studied perovskite as ceramic pigment structure:

(i) Eppler [1] develops black pigments from $(Sr,Ca)MnO_3$ perovskites using oxides and carbonates mixed with conventional mineralizers fired at 730 °C with soaking time of 3 h.
(ii) Pishch I and Radion [2] applies the $(NiCa)TiO_3$ perovskite as yellow pigment and $(CoCa)TiO_3$ as brown-turkish colorations using precipitation synthesis methods. Yellow shade increasing when Ni increase is associated to a shifting of Ni(II) bands absorption in octahedral coordination. Yellow application is limited and cobalt blue based pigment is really a solution colorant. Likewise these authors use $MTiO_3$ and $MZrO_3$ (M = Ca, Sr, Cd, Zn) perovskites obtained from alkaline precipitation with 1 M NaOH 1 M as white ceramic pigments [3].
(iii) Jansen and Letschert [4] pose an alternative to cadmium sulfoselenide included into zircon pigment based on nitride solid solutions $CaTaO_{2+x}N_{1-x}$ and $LaTaO_{2+x}N_{1-x}$ that change from yellow to orange and red, in function of N amount in perovskite solid solution (as cadmium sulfoselenide in zircon in function of Cd amount). Cadmium sulfoselenide in zircon pigment does not show toxicity due to their low solubility, but it may promote biodisposal cadmium when is deposited as waste or incinerated, is for that because their use has been restricted. Although the use of cadmium sulfoselenide included into zircon pigment, may be considered sure from recently studies, there is high interest to dispose an alternative. Rare earth presence on perovskites is not a problem, but oxynitride synthesis, by ammonolisis of oxide mixture at high temperature and soaking times, is more complicated than for cadmium sulfoselenide in zircon pigment, and stability on ceramic matrices and glazes is lower than cadmium-zircon pigment also, but it is a stable alternative for polymer colouration [5].

Kim et al. [6] study crystallographic features of AMO_2N (A = Ba, Sr, Ca; M = Ta, Nb) oxynitride perovskites: $BaTaO_2N$ structure becomes cubic (distance Ta–O/N = 2.056 Å), $SrTaO_2N$ and $CaTaO_2N$ show octahedral distortion showing lower distances Ta–O/

* Corresponding author. Tel.: +34 0964 728250; fax: +34 0964 728214.
E-mail address: monros@qio.uji.es (G. Monrós).

0272-8842/$36.00
doi:10.1016/j.ceramint.2011.06.027

N = 2.02 Å. Nb oxinitrides are isostructural with above homologous Ta perovskites with Nb–O/N distances slightly higher. The estimated band-gap from diffuse reflectance studies are: $BaTaO_2N$, 1.8 eV; $SrTaO_2N$, 2.1 eV; $CaTaO_2N$, 2.4 eV; $BaNbO_2N$, 1.8 eV; $SrNbO_2N$, 1.9 eV; $CaNbO_2N$, 2.1 eV. Impedance spectroscopy and electric transport measurements indicate that $BaNbO_2N$ shows metallic conductivity (probably by reduction during sintering) instead tantalates are semiconductors. Likewise, Cheviré et al. [7] studied optical properties of $La_{1-x}A_xTiO_{2+x}N_{1-x}$ (A = Sr, Ba) systems obtained by ammonolisis at 950 °C from fused salts as precursors.

(iv) Stobierska et al. [8] and Matteucci et al. [9] obtain Cr and other chromophores doped $YAlO_3$ and characterize their performance in several ceramic matrices and glazes.

Therefore perovskite becomes a ceramic structure that must be added to DCMA list of ceramic pigments [10]. Other perovskites based on neodymium and titanium can be used as ceramic pigments [11].

In the other hand, the structural stability of a ceramic pigment into the matrix becomes associated to three main principles [12]: (a) valence changeability of the chromophore ion; versatile ion valence of chromium (III, IV, V and VI valence) or vanadium (III, IV and V valence) make them interesting chromophore and catalytic ions, (b) diffusion capacity of the chromophore ion into host crystal; in this sense there are ceramic pigments such as chrome-alumina or manganese-alumina than can be obtained by direct reaction between the chromophore and oxides, but in other cases such as chromium-sphene (Cr-$CaSnSiO_5$) or zircon based pigments (vanadium turquoise, pink koral and yellow of praseodymium) the crystal phase host and pigment must be prepared simultaneously, and it is well known that on the first case the pigmenting properties resides on the doped surface of the host phase particles, (c) stability of the chromophore substitution against other dopants that can be present on the ceramic matrices; it is the case of decolouring of blue or black pigments based on Co–Al, Co–Fe and Co–Ni spinels in rich zinc content glazes which interacts with spinel precipitating the high stable gahnite phase ($ZnAl_2O_4$).

Vanadium is the chromophore agent in several ceramic pigments listed by DCMA: vanadium-zirconia yellow (1-01-4), vanadium-antimony in rutile grey (11-21-8), vanadium cassiterite yellow (11-22-4) and vanadium zircon turquoise (14-42-2).

Lin et al. [13] study the effects of vanadium doping on resistive switching characteristics and mechanisms of magnetron RF-sputtered $SrZrO_3$ perovskite based thin films and propose that the Zr^{4+} sites might be substituted by V^{5+} when vanadium doped into $SrZrO_3$ perovskite thin films, because the ion radius of V^{5+} (0.54 Å of effective radius for VI coordination) is much closer to Zr^{4+} (0.72 Å for VI coordination) than Sr^{2+} (1.18 and 1.44 Å for VI and XII coordination index respectively) [14]. Therefore, a decrease in the lattice constants of $SrZrO_3$ perovskite with increasing vanadium doping concentration up to 0.2 mol% is observed, whereas the lattice constants of 0.2, 0.3, and 0.4 mol% V:$SrZrO_3$ thin films are almost equal. Based on Vegard's law, the lattice constants of the films change with the concentration of vanadium up to 0.2 mol%, i.e., the concentration less than 0.2 mol% is within the solid solubility limit. The conduction mechanisms of $SrZrO_3$ perovskite based thin films are dominated by ohmic conduction (hoping conduction) and Frenkel–Poole emission for the low resistance state (LRS) and the high resistance state (HRS), respectively. The turn-on process might be attributed to the formation of conducting filaments consisting of oxygen vacancies with the effective barrier height in the range of 0.10–0.13 eV, whereas the turn-off process might result from thermally assisted oxidation of oxygen vacancies by the Joule heating effect. Furthermore, the introduction of the high valence cation V^{5+} in a Zr^{4+} site $SrZrO_3$ perovskite crystalline structure can suppress the formation of oxygen vacancies due to the charge neutrality restriction.

In the other hand Reddy et al. [15] study the effect of V_2O_5 on CaO–TiO_2 catalysts and their activity for cyclohexanol conversion. The CaO–TiO_2 binary oxide (1:1 molar ratio) was synthesized by a homogeneous co-precipitation method from ultrahigh dilute solutions of the corresponding chlorides and calcined at various temperatures from 723 to 1273 K. On the fired CaO–TiO_2 support (723 K) various amounts of V_2O_5 (2.5–10 wt.%) were deposited from ammonium metavanadate by a wet impregnation method and calcined at different temperatures. Conversion of cyclohexanol to cyclohexanone/cyclohexene was performed as a model reaction to assess the acid–base properties of the prepared catalysts. The CaO–TiO_2 mixed oxide contains mainly anatase phase and at higher calcination temperatures some portions of this mixed oxide is converted into $CaTiO_3$ and is thermally quite stable up to 1273 K. The CaO–TiO_2 binary oxide results a promising support for V_2O_5 dispersion. Impregnated V_2O_5 remains in a highly dispersed and amorphous state over the support and the dispersion behaviour is dependent upon the vanadia loading. In particular, the formation of $CaVO_3$ compound in the case of V_2O_5/CaO–TiO_2 samples as inferred by XRD and XPS observations, inhibits the formation of the most feasible $V_xTi_{(1-x)}O_2$ (rutile solid solution) at higher calcination temperatures. Finally authors concluded that the CaO–TiO_2 mixed oxide exhibits more cyclohexanone selectivity and V_2O_5/CaO–TiO_2 more cyclohexene selectivity in the conversion of cyclohexanol reflecting their basic and acidic properties, respectively.

Perovskite, $CaTiO_3$, shows mixed ionic and electronic conductivity at low oxygen partial pressure and maintains its structure in the presence of high concentrations of defects [16]. Substitution of calcium titanate by acceptor impurities in Ti-sites improves both ionic and electronic conductivity [17]. The most considerable increase of the electrical conductivity is achieved by iron-substitution, which makes this material particularly attractive for use as a membrane for hydrogen production. The samples of the system $CaTi_{1-x}Fe_xO_{3-\delta}$ ($x = 0$, 0.1. . .0.5) were synthesized by solid-state reaction of the corresponding oxides or carbonates by Dunyushkina [17]. These materials were weighed in the defined molar ratio and mixed in an agate mortar under ethyl alcohol for about 30–

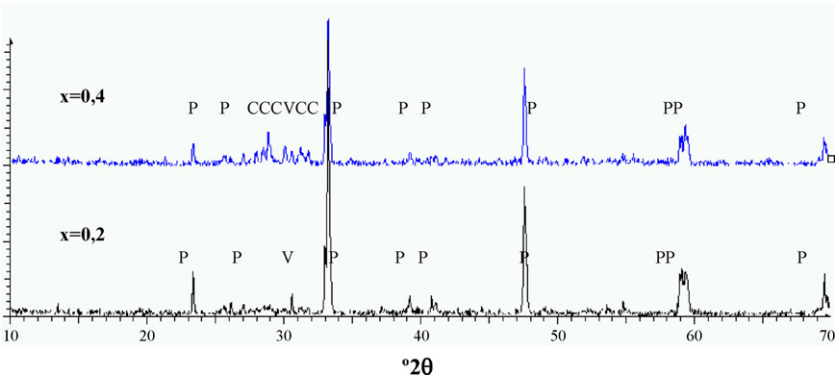

Fig. 1. XRD evolution of $Ca(V_xTi_{1-x})O_3$ samples with x: P(perovskite $CaTiO_3$), V(V_6O_{11}), C(CaV_2O_7).

40 min. The homogeneous powders were pressed and heated at a rate of 5 °C/min to a temperature of 1200 °C where they were kept for 2 h. The fired pellets were ground again, pressed for the second time, heated at the same rate to 1470 °C and exposed for 2 h. According to X-ray diffraction analysis results all samples were single-phase and exhibited orthorhombic symmetry.

In this paper a new pink vanadium doped calcium titanate $Ca(V_xTi_{1-x})O_3$ ceramic pigment in conventional ceramic glazes is obtained by ceramic route and characterized.

2. Experimental

Vanadium doped calcium-titanium perovskite $Ca(V_xTi_{1-x})O_3$ $x = 0.2$, 0.3 and 0.4 and mixed iron-vanadium calcium-titanium perovskite $Ca(V_xFe_xTi_{1-x})O_3$ $x = 0.1$, 0.2 and 0.3 have been prepared by ceramic method. In this method, calcium carbonate $CaCO_3$, vanadium metavanadate NH_4VO_3, iron oxide Fe_2O_3 and anatase TiO_2, all supplied by Panreac S.A., have been used as precursors to 20 g of final product, ceramic mixture were milled in acetone medium, and fired at 1000 °C with 3 h of soaking time.

Samples have been characterized by several techniques:

(a) X-ray diffraction (XRD) carried out on a Siemens D5000 diffractometer using Cu K_α radiation, 20–70° 2θ range, scan rate 0.05° 2θ/s, 10 s per step and 40 kV and 20 mA conditions.
(b) Microstructure characterization of powders was carried out by scanning electron microscopy (SEM), using a Leo-440i microscope supplied by LEYCA. Likewise SEM-EDX microstructural analysis was obtained in a LEO-440i electronic microscope equipped by a microanalysis system supplied by Oxford.
(c) UV–vis–NIR spectra of 5% weight glazed samples in a conventional SiO_2–CaO–ZnO glaze for double firing stoneware have been collected using a Lambda 2000 spectrometer supplied by Perkin Elmer through diffuse reflectance technique. L*a*b* colour parameters of, glazed samples were measured following the CIE (Commission International de l'Eclairage) colorimetric method [18] using a Perkin-Elmer spectrophotometer, with standard lighting C. On this method, L* is a measure of brightness (100 = white, 0 = black) and a* and b* of chroma (−a* = green, +a* = red, −b* = blue, +b* = yellow).
(d) Specific surface analyser Gemini V equipped with Flow Prep 060 gas desorption system supplied by Micromeritics was used for specific surface measurements B.E.T. [19] of samples.
(e) Cell parameters measurements have been carried out using α-Al_2O_3 as internal standard and indexation of XRD peaks by POWCAL and LSQC programmes [20].

3. Results and discussion

XRD evolution of crystalline phases in ceramic samples and CIEL*a*b* of fired powders 5% glazed in a CaO–ZnO–SiO_2 conventional glaze in function of vanadium amount used as raw material are shown in Fig. 1 and Table 1 respectively. XRD in Fig. 1 indicate the crystallization of the perovskite $CaTiO_3$ as the main crystalline phase together with very weak peaks that can be associated to V_6O_{11} phase in the $x = 0.2$ sample. In $x = 0.3$ (not shown) and $x = 0.4$ samples XRD peaks associated to $Ca_2V_2O_7$ calcium pyrovanadate, that increase with x, are detected also. These results indicate that the limit of solid solution of vanadium in $Ca(V_xTi_{1-x})O_3$ lattice is further down than $x = 0.2$ and excess of vanadium reacts with calcium to produce $Ca_2V_2O_7$ decreasing the amount of perovskite crystallization.

CIEL*a*b* colour measurement of fired powders 5% glazed in a CaO–ZnO–SiO_2 conventional glaze of $Ca(V_xTi_{1-x})O_3$ $x = 0.2$, 0.3 and 0.4 samples in Table 1 indicate that the intensity of colour diminish (L* increase) when x increase. Likewise a* and b* parameters diminish when x increase, indicating that both red and yellow shade decreasing when x increase. The $x = 0.2$ sample shows the best pink colour obtained when it is 5% glazed into the double firing CaO–ZnO–SiO_2 conventional

Table 1
CIEL*a*b* colour parameters of $Ca(V_xTi_{1-x})O_3$ samples fired at 1000 °C/3 h with x: 5% glazed in a conventional double firing stoneware glaze.

x	L*	a*	b*
0.2	63.6	11.2	31.1
0.3	64.5	10.4	23.5
0.4	69.9	7.2	14.3

glaze (L*a*b* = 63,6/11,2/31,1). This result agrees with XRD data because in $x = 0.3$ and $x = 0.4$ samples the crystallization of $Ca_2V_2O_7$ dilute the real amount of saturated $Ca(V_xTi_{1-x})O_3$ solid solution in the glazed sample.

The unit cell parameter measurements of $Ca(V_xTi_{1-x})O_3$ $x = 0.2$ sample shown in Table 2 indicate that the entrance of vanadium into perovskite lattice diminish c parameter and the cell volume of perovskite decreases. This result agrees with literature [13]: the Ti^{4+} sites might be substituted by V^{5+} when vanadium doped into $CaTiO_3$ perovskite because the ion radius of V^{5+} (0.54 Å of effective radius for VI coordination number [14]) is much closer to Ti^{4+} (0.605 Å for VI coordination) than Ca^{2+} (1.00 and 1.34 Å for VI and XII coordination index respectively). Furthermore, the introduction of the high valence cation V^{5+} in a Ti^{4+} site $CaTiO_3$ perovskite crystalline structure suppress the formation of oxygen vacancies in order to preserve the charge neutrality restriction of the lattice, limiting the solid solution.

UV–vis–NIR spectra of 5% weight glazed $Ca(V_xTi_{1-x})O_3$ $x = 0.2$, 0.3 and 0.4 samples in a conventional SiO_2–CaO–ZnO glaze for double firing stoneware collected through diffuse reflectance technique are shown in Fig. 2. Two broad bands centred at 320 nm and 420 nm can be observed and associated to charge transfer band Ti^{4+}–$O^{=}$ and V^{5+}–$O^{=}$ respectively. This V^{5+}–$O^{=}$ charge band transfer produces the pink colour in agreement with CIEL*a*b* measurements and XRD results: its intensity diminish with x but its wavelength position does not change (420 nm), indicating a diminution of real amount of pigment in $x = 0.3$ and $x = 0.4$ glazed samples due to the crystallization of $Ca_2V_2O_7$. The fundamental absorption on V_2O_5 (space group Pmmn) is found at 530 nm [21] whit V^{5+} in distorted trigonal bipyramidal coordination (CN=V). In the $Ca(V_xTi_{1-x})O_3$ solid solution, V^{5+} shows octahedral coordination and the increase of the oxygen crystal field shifts the absorption to 420 nm.

Measured B.E.T. specific surface for $x = 0.2$ sample is 0.59 m^2/g. SEM micrographs and EDX mapping of $Ca(V_xTi_{1-x})O_3$ $x = 0.2$ sample are shown in Figs. 3 and 4 respectively. Fig. 3a indicates the existence of aggregates of particles in the range 5–25 μm of size, and Fig. 3b shows that the aggregates are built by spherical particles with sintering necks with a size between 1 and 4 μm. The EDX mapping of $Ca(V_xTi_{1-x})O_3$ $x = 0.2$ sample shown in Fig. 4 indicates a homogeneous distribution of doped vanadium on the perovskite particles, in agreement with the formation of a solid solution.

As mentioned above, the introduction of the high valence cation V^{5+} in a Zr^{4+} site $SrZrO_3$ perovskite crystalline structure suppress the formation of oxygen vacancies due to the charge neutrality restriction of the lattice. In order to avoid this limitation, Fe^{3+} and V^{5+} codoped samples $Ca(Fe_xV_xTi_{1-2x})O_3$ $x = 0.1$, 0.2 and 0.3 have been prepared following the ceramic route described above and also fired at 1000 °C with 3 h of soaking time. The obtained powders show a brown colour, their UV–vis–NIR optical reflectance spectra are shown in Fig. 5

Table 2
Unit cell parameter measurements of $Ca(V_xTi_{1-x})O_3$.

x	a (Å)	b (Å)	c (Å)	V (Å^3)
0	5.44050	7.64360	5.38120	223.78
JCPDS 22-153				
0.2	5.441(3)	7.644(4)	5.370(6)	223.34

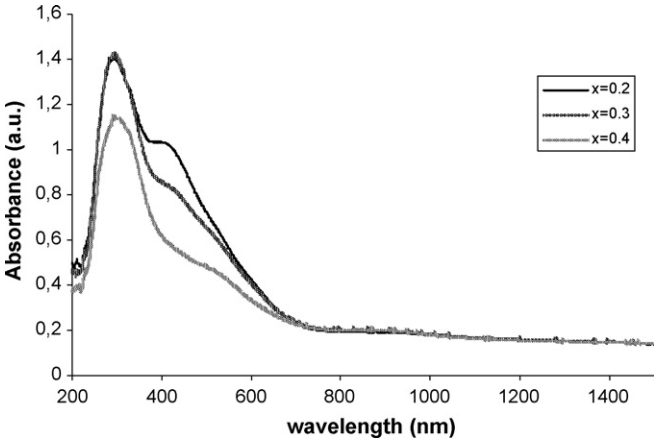

Fig. 2. UV–vis–NIR spectra of $Ca(V_xTi_{1-x})O_3$ $x = 0.2$, 0.3 and 0.4 indicated samples.

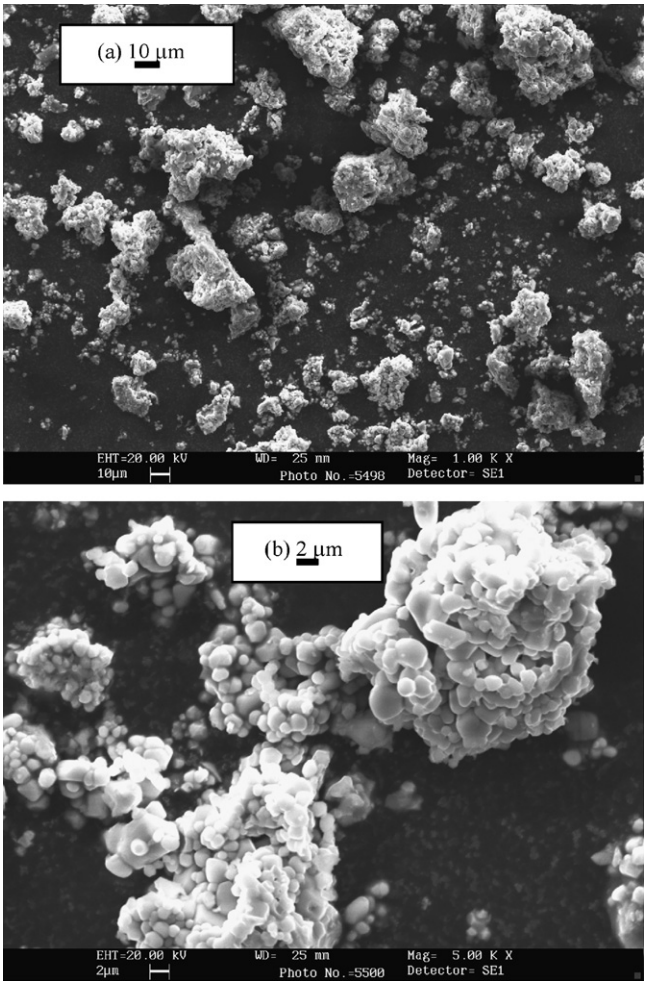

Fig. 3. SEM micrographs of $Ca(V_xTi_{1-x})O_3$ $x = 0.2$ sample.

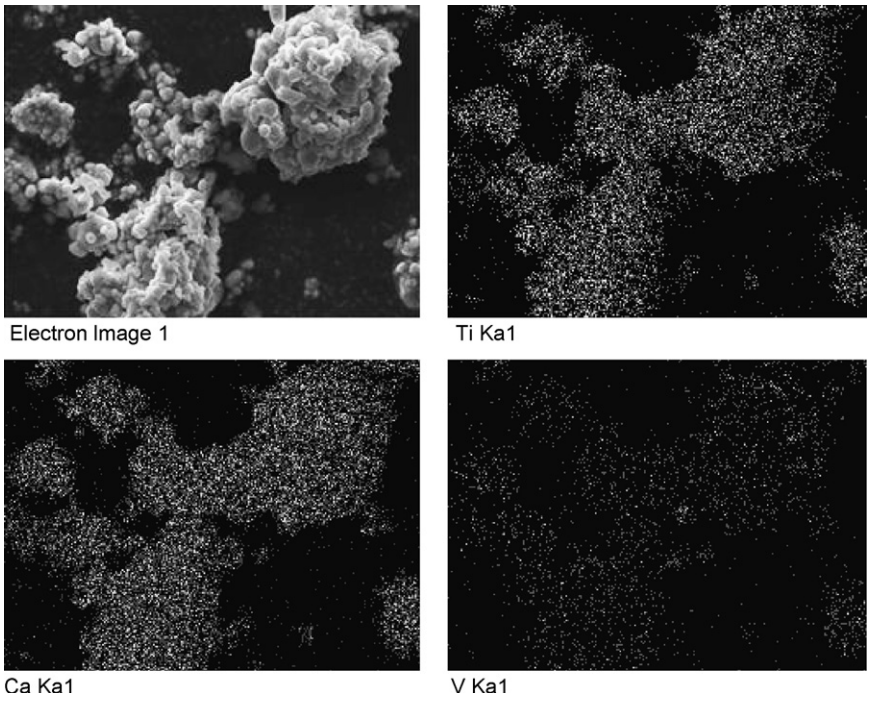

Fig. 4. EDX mapping of $Ca(V_xTi_{1-x})O_3$ $x = 0.2$ sample.

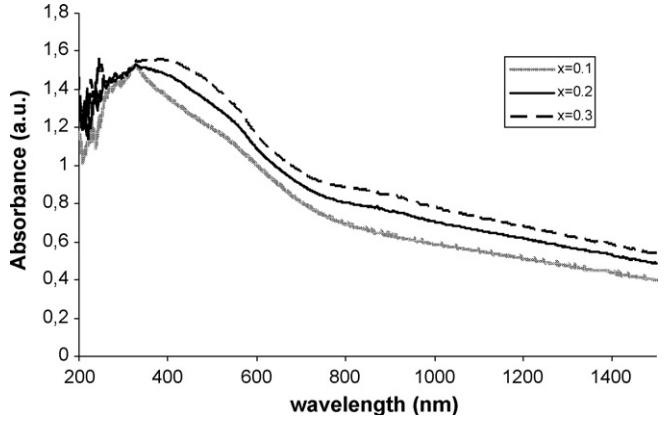

Fig. 5. UV–vis–NIR spectra of $Ca(Fe_xV_xTi_{1-2x})O_3$ $x = 0.1$, 0.2 and 0.3 indicated samples.

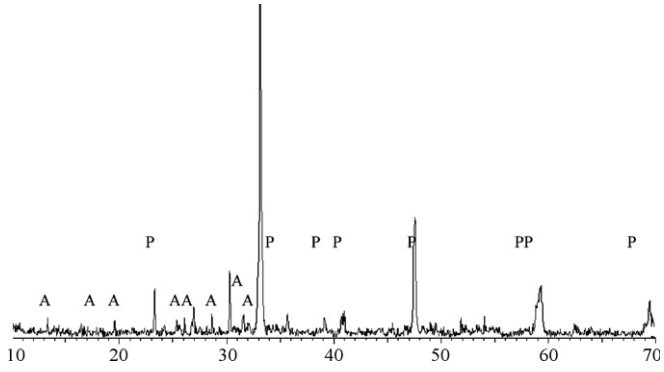

Fig. 6. XRD diffractogram of $Ca(Fe_xV_xTi_{1-2x})O_3$ $x = 0.2$.

where broad bands at 380, 580 and 900 nm can be observed. However fired powders 5% glazed in a CaO–ZnO–SiO_2 conventional glaze do not produce colour. Therefore codoped iron inhibits the pigmenting capacity of vanadium doped perovskite. XRD diffractogram of $Ca(Fe_xV_xTi_{1-2x})O_3$ $x = 0.2$ is shown in Fig. 6: Intense XRD peaks associated to perovskite are detected together medium peaks of calcium orthovanadate ($Ca_3V_2O_8$): iron-perovskite solid solution [17] has been obtained but calcium orthovanadate keeps vanadium avoiding its entrance in perovskite solid solution pigment.

4. Conclusions

A new pink vanadium doped calcium titanate $Ca(V_xTi_{1-x})O_3$ ceramic pigment in SiO_2–CaO–ZnO conventional ceramic glazes has been obtained by ceramic route. The solid solution limit is near by $x = 0.2$, higher amounts of vanadium crystallizes $Ca_2V_2O_7$ which dilute the real amount of saturated $Ca(V_xTi_{1-x})O_3$ solid solution and diminish the colour intensity.

The unit cell parameter measurements of $Ca(V_xTi_{1-x})O_3$ $x = 0.2$ indicate that the entrance of vanadium into perovskite lattice diminish c parameter and the cell volume of perovskite decreases. This result agrees with the substitution of Ti^{4+} by V^{5+} when vanadium enters into $CaTiO_3$ perovskite lattice.

UV–vis–NIR spectra of 5% weight glazed $Ca(V_xTi_{1-x})O_3$ $x = 0.2$, 0.3 and 0.4 samples show a broad band centred at 320 nm associated to charge transfer bands Ti^{4+}–$O^{=}$ and other at 420 nm associated to V^{5+}–$O^{=}$ charge transfer that explain the pink colour obtained. V^{5+} in octahedral coordination field shifts the absorption from 530 nm in V_2O_5 (V^{5+} in distorted trigonal bipyramidal coordination) to 420 nm.

SEM–EDX indicates that $Ca(V_xTi_{1-x})O_3$ $x = 0.2$ sample fired 1000 °C with 3 h of soaking time shows a low sintering step of particles between 1 and 4 μm of size that form aggregates between 5 and 25 μm with a specific surface of 0.59 m^2/g.

In order to avoid the limitation due to the suppressing of oxygen vacancies by high valence cation V^{5+} substitution in a Ti^{4+} site $CaTiO_3$ perovskite for to preserve the charge neutrality of the lattice: Fe^{3+} and V^{5+} codoped samples $Ca(Fe_xV_{x-}Ti_{1-2x})O_3$ $x = 0.1$, 0.2 and 0.3 have been prepared showing a brown colour when fired ad 1000 °C during 3 h, but 5% glazed in a $CaO–ZnO–SiO_2$ conventional glaze do not produce colour, indicating that codoped iron inhibits the pigmenting capacity of vanadium doped $CaTiO_3$ perovskite.

Acknowledgement

Authors acknowledge the financial support given by FUNDACION CAJA CASTELLÓN-UJI, P1-1B2010-09 project.

References

[1] R.A. Eppler, Black Pigments Free of Heavy Metals, US Patent 06/357959 (1983).
[2] I.V. Pishch I, E.V. Radion, Production of white pigments based on zirconates and titanates using the precipitation method, Glass Ceram. 55 (1998) 9–10.
[3] I.V. Pishch I, E.V. Radion, Synthesis of pigments based on perovskite, Glass Ceram. 63 (1) (2006) 55–58.
[4] M. Jansen, H.P. Letschert, Inorganic yellow-red pigments without toxic metals, Nature 404 (2000) 980–982.
[5] G. Tobías, Doctoral These, Nuevos oxinitruros laminares de niobio y tántalo y sistemas relacionados, Universitat Autónoma de Barcelona, 2004.
[6] Y.-I. Kim, P.M. Woodward, K.Z. Baba-Kishi, C.W. Tai, Characterization of the structural, optical, and dielectric properties of oxynitride perovskites AMO_2N (A = Ba, Sr, Ca; M = Ta, Nb), Chem. Mater. 16 (7) (2004) 1267–1276.
[7] F. Cheviré, F. Tessier, R. Marchand, Optical properties of the perovskite solid solution $LaTiO_2N–ATiO_3$(A = Sr, Ba), Eur. J. Inorg. Chem. 6 (2006) 1223–1230.
[8] E. Stobierska, J. Lis, M.M. Bućko, A. Gubernat, Ceramic pigments with perovskite structure, Adv. Sci. Technol. 45 (2006) 276–280.
[9] F. Matteucci, C. Lepri Neto, M. Dondi, G. Cruciani, G. Baldi, A.O. Boschi, Colour development of red perovskite pigment $Y(Al,Cr)O_3$ in various ceramic applications, Adv. Appl. Ceram. 105 (2) (2006) 99–106.
[10] DCMA Classification and Chemical Description of de Mixed Metal Oxide Inorganic Coloured Pigments, 2nd ed., Metal Oxides and Ceramic Colours Subcommitee, Dry Color Manufacturer's Assn., Washington, D.C., 1982.
[11] C. Gargori, R. galindo, M. Llusar, S. Cerro, A. García, G. Monrós, Chromium-calcium titanate red ceramic pigment, Adv. Sci. Technol. 68 (2010) 208–212.
[12] F. Ren, S. Ishida, N. Takeuchi, Chromium-based ceramic colors, Ceram. Bull. 71 (1995) 759–764.
[13] M.-H. Lin, M.-C. Wu, C.-H. Lin, T.-Y. Tseng, Effects of vanadium doping on resistive switching characteristics and mechanisms of $SrZrO_3$-based memory films, IEEE Trans. Electron Devices 57 (8) (2010) 1801–1808.
[14] R.D. Shannon, C.T. Prewit, Effective ion radii in oxides and fluorides, Acta Crystallogr. 8 (1969) 925–945.
[15] B.M. Reddy, K.J. Ratnam, P. Saikia, Characterization of $CaO–TiO_2$ and $V_2O_5/CaO–TiO_2$ catalysts and their activity for cyclohexanol conversion, J. Mol. Catal. A: Chem. 252 (2006) 238–244.
[16] W.L. George, R.E. Grace, Formation of point defects in calcium titanate, J. Phys. Chem. Sol. 30 (1969) 881–887.
[17] L.A. Dunyushkina, A.K. Demin, B.V. Zhuravlev, Electrical conductivity of iron-doped calcium titanate, Solid State Ionics 116 (1999) 85–88.
[18] CIE Commission International de l'Eclairage, Recommendations on Uniform Color Spaces, Color Difference Equations, Psychometrics Color, Terms, Supplement n° 2 of CIE Pub. N° 15, (E1-1.31) 1971, Bureau Central de la CIE, Paris, 1978.
[19] S. Brunauer, P.H. Emmett, E. Teller, Adsorption of gases in multimolecular layers, J. Am. Chem. Soc. 60 (1938) 309–319.
[20] POWCAL and LSQC Programmes, Dpt. of Chemistry, University of Aberdeen, UK.
[21] C.V. Ramana, B.S. Naidu, O.M. Hussain, R. Pinto, Low-temperature growth of vanadium pentoxide thin films produced by pulsed laser ablation, J. Phys. D: Appl. Phys. 34 (7) (2001) L35–L38.